

## Chapter 2

# Introduction to Neutrino Physics

In neutrino physics many exciting discoveries have been made in the last decades. Most importantly, the discovery of neutrino oscillations, first indicated by the Homestake experiment [1, 2] and finally validated by Super-Kamiokande in 1998 [3] and SNO in 2001 [4, 5]. With the help of an impressive suite of atmospheric, solar, reactor and accelerator neutrino experiments most of the free parameter space of neutrino oscillation could be determined. However, only in June 2011 a first hint of a non-zero value of the remaining undetermined mixing angle  $\theta_{13}$  was found by T2K in Japan [6] and more recently by the Double Chooz experiment [7].

Despite many fundamental discoveries in neutrino physics the elusive “ghost particle of the universe” still provides many burning open questions. In the Standard Model the neutrino is assumed to be massless. The discovery of neutrino oscillations, however, has proven that the neutrino is not massless in nature. In this context, single  $\beta$ -decay experiments were aimed to determine the absolute neutrino mass and could show that it is at least lighter by a factor of  $10^5$  compared to the electron mass. This factor gives rise to the puzzling question of how the neutrino acquires mass.

A closely related open question is the nature of the neutrino with respect to the CP-symmetry operator, i.e. whether it is a Majorana particle or a Dirac particle. Experiments looking for neutrinoless double  $\beta$ -decay are ideally suited to answer this question.

Neutrino oscillations depend on the mass splittings  $\Delta m_{ij}^2$  between the three mass eigenstates of the neutrino. The parameters  $\Delta m_{12}^2$  and  $\Delta m_{23}^2$  have been measured by several oscillation experiments to rather good accuracy. However, so far, the sign of  $\Delta m_{23}^2$  is still undetermined. Therefore, the hierarchy of the neutrino masses is still not known.

Finally, the absolute mass scale of the neutrino is so far only constrained by single  $\beta$ -decay experiments, with the most sensitive experiments at Mainz and Troitsk setting an upper limit of 2 eV [8–11]. Cosmology and the search for neutrinoless double  $\beta$ -decay can provide more stringent bounds, however, these results are much more model dependent. As the knowledge of the absolute neutrino mass scale is

an extremely important input both for cosmological models and for the fundamental understanding of the nature of the mass, all three methods complement each other.

This chapter gives an overview of neutrino physics. In Sect. 2.1 a brief history of the discovery of the neutrinos is given. In Sect. 2.2 the principle and status of neutrino oscillations is presented. Section 2.3 describes the minimal extensions of the Standard Model, that allow for introducing a neutrino mass term. Finally, the three major approaches to determine the neutrino mass will be discussed in Sect. 2.4.

## 2.1 The Discovery of the Neutrino

The neutrino was part of theoretical physics long before it was actually detected. After Pauli postulated it, a period of 26 years passed until it was detected by project Poltergeist, fortunately still during Pauli's lifetime. In the following these two landmarks, Pauli's postulate and the experimental discovery of neutrinos of all flavors, will be outlined.

### 2.1.1 Postulation of the Neutrino by Pauli

When the energy spectrum of  $\beta$ -decay electrons was first investigated in 1914 by James Chadwick [12], he expected to measure a mono-energetic line of the electron, owing to the then assumed two-body decay nature. However, a continuous spectrum was observed, as shown in Fig. 2.1. This observation is in contradiction to energy and angular momentum conservation if a two-body decay is assumed. In his famous Letter dated to the 4th of December 1930, Pauli [13] postulated the existence of a neutral spin  $\frac{1}{2}$  particle, the “neutron”, which is produced in  $\beta$ -decays alongside the charged electron. In that case the  $\beta$ -decay can be described as three-body decay, and the contradictions to conservation laws are resolved. When the neutron was two years

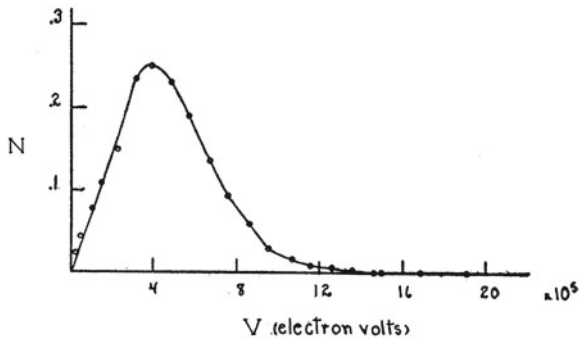


**Fig. 2.1** Continuous energy spectrum of the beta electrons from radium decay [15]

later found, however, it was clear that due to its large mass this particle could not be the missing neutral particle in the  $\beta$ -decay. In 1934, E. Fermi, who theoretically described the  $\beta$ -decay, introduced the name “neutrino” for Pauli’s hypothetical particle [14]. Fermi derived an expression for the shape of the electron energy spectrum, and, from comparison with available data deduced that the neutrino mass must be either zero or much smaller than the electron mass.

### 2.1.2 First Detection of a Neutrino

The first detector that “saw” the neutrino was the detector “Herr Auge” (see Fig. 2.2a) located at the Hanford reactor site as the centerpiece of the famous project Poltergeist by C. Cowan and F. Reines. However, the background in this 1954 pioneering experiment was still overwhelming the signal. Shortly after these initial studies, C. Cowan and F. Reines could definitively prove the existence of the neutrino with an improved detector (see Fig. 2.2b) at the Savannah river reactor [16, 17]. The neutrino was detected by the classical inverse  $\beta$ -decay

$$\bar{\nu}_e + p \rightarrow n + e^+. \quad (2.1)$$

The Savannah River detector consisted of liquid scintillator tanks inter spaced with a Cadmium-loaded (Cd) water target. The positron from Eq. (2.1) annihilates with an electron, giving rise to a prompt signal of two back to back gammas. The neutron is thermalized on a timescale of milliseconds and finally captured by Cd, thereby releasing gammas when the excited Cd-state decays to the ground state

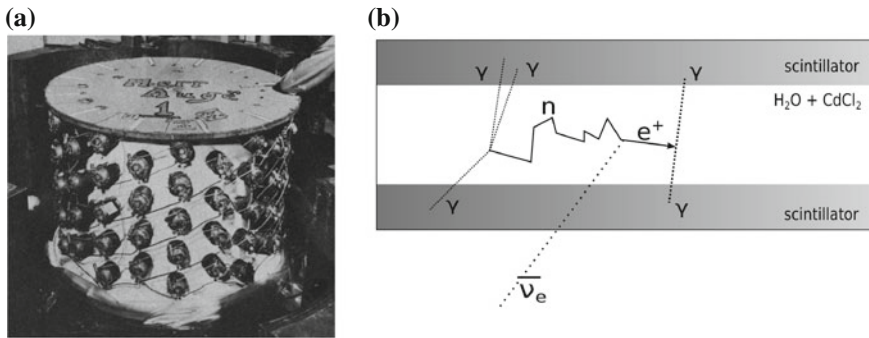


**Fig. 2.2** First neutrino detector and detection principle. **a** Photograph of the first neutrino detector named “Herr Auge”, Source [16]. **b** Detection principle: the antineutrino  $\bar{\nu}_e$  from the reactor hits a free proton in the  $\text{H}_2\text{O} + \text{CdCl}_2$  target thereby producing a positron and a neutron. The positron annihilates, while the neutron is captured on cadmium after moderation. The subsequent gammas are detected by Compton scattering in the liquid scintillation detector. The scintillation light is detected by photomultipliers

(see Fig. 2.2b). These gammas are detected by their subsequent Compton scattering. The scintillation light is detected by photomultiplier tubes surrounding the detector volume. The prompt and the delayed light signal represent a distinct coincidence signature of a neutrino interacting in the detector. Long after this crucial discovery, the Nobel Prize was given to F. Reines in 1995 for the first detection of the neutrino.

### 2.1.3 Discovery of $\nu_\mu$ and $\nu_\tau$

The second neutral lepton flavor state, the muon neutrino  $\nu_\mu$  was found by L.M. Lederman, M. Schwartz and J. Steinberger in 1962 at the Brookhaven Alternating Gradient Synchrotron (AGS) [18]. There, neutrinos from pion decay

$$\pi^+ \rightarrow \mu^+ + \nu_\mu \quad (2.2)$$

were investigated. To identify the  $\nu$ -flavor associated with the  $\pi$ -decay, the flavor of the charged lepton, being produced via a charged current interaction in the detector, had to be detected. For this purpose a spark chamber made of 10 t of aluminum was used. As only tracks from muons and no electronic showers were observed, the conclusion was, that the neutrinos produced together with a muon, i.e. muon neutrinos, are intrinsically different from electron (anti-)neutrinos. For the discovery of a second kind of neutrino the three were awarded with the Nobel prize in 1988.

Finally, in the year 2000, the tau neutrino  $\nu_\tau$  was detected in the Direct Observation of Nu Tau (DONUT) experiment at Fermilab [19]. In this experiment a beam of 800 GeV protons impinged on to a tungsten target to create a particle shower. A small fraction of the particles decays into  $\tau$  leptons, which in turn produce  $\nu_\tau$  when they decay. With a massive shielding all particles but the  $\nu_\tau$  were removed. The  $\nu_\tau$ 's are detected in an emulsion lead target. When interacting in the lead they produce a  $\tau$  lepton, which, due to its short lifetime, produces a short track in the emulsion. All decay products, but the neutrino, leave a track in the emulsion with a different direction than the  $\tau$ . The famous signature of  $\tau$  neutrinos is therefore a “kink” in the particle tracks.

Already in 1989, the three generation picture with  $N_\nu = 3$  was established by the ALEPH experiment at the LEP collider at CERN. This was based on the precise measurement of the invisible width of the Z boson resonance at 91 GeV [20, 21].

## 2.2 Neutrino Oscillations

The discovery of neutrino oscillations is a crucial milestone for neutrino physics with far reaching implications for particle physics and cosmology. It proves that the neutrinos are not massless, since it requires the neutrino mass eigenstates to have different masses. Assuming the lightest neutrino  $\nu_1$  being (almost) massless,

the measurement of the mass splittings gives a lower mass bound. In this section the discovery of neutrino oscillation, the standard theoretical treatment and the neutrino oscillations in matter will be described.

### 2.2.1 First Discovery

In the second half of the 1960s physicists and nuclear chemists started seriously thinking about measuring neutrinos from the sun. In nuclear fusion processes, i.e. in the pp-chain and the sub-dominant CNO-cycle [22], neutrinos with exclusively electron-type flavor are produced. The flux of solar neutrinos at the distance of the earth equals to about 60 billion neutrinos per  $\text{cm}^2$  and second. Figure 2.3 shows the energy spectrum of the neutrinos being produced in the solar core. In contrast to reactors, the pp and CNO cycles in the sun only produce electron neutrinos  $\nu_e$  (i.e. no electron anti neutrinos  $\bar{\nu}_e$ ).

In the first solar neutrino experiment, the Homestake experiment led by Ray Davis Jr. [1, 2], the radiochemical detection technique was pioneered. Homestake was based on a tank of 600 t of perchloroethylene, containing the isotope  $^{37}\text{Cl}$  as neutrino target. The  $^{37}\text{Cl}$  nucleus, when interacting with a  $\nu_e$  from the sun

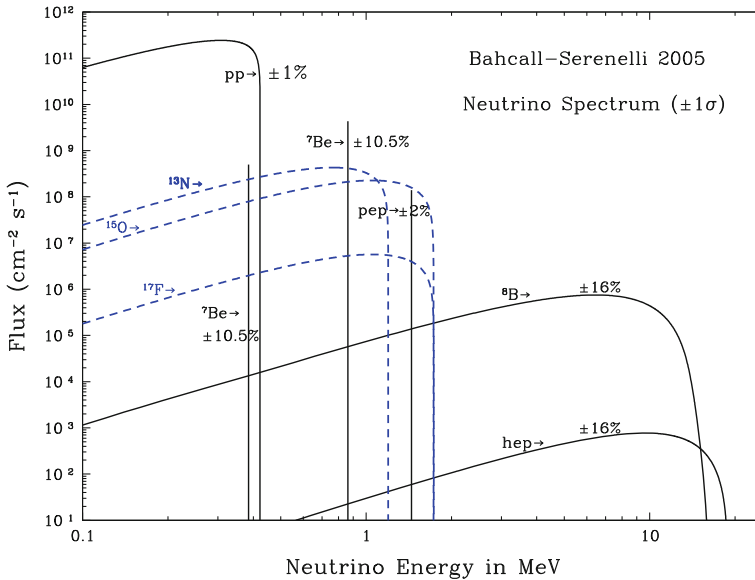


**Fig. 2.3** Solar neutrino spectrum. In this plot the flux of neutrinos from the pp-chain (*solid line*) and the CNO cycle (*dashed lines*) are shown as a function of energy. The integral spectrum is measured down to 0.2 MeV by e.g. Gallex and SAGE. Experiments measuring a differential spectrum have a higher threshold. SNO detects  $E_\nu > 6$  MeV, Borexino [23, 24] can reach below 1 MeV [25]

is transmuted into an excited  $^{37}\text{Ar}$  atom. After a measuring interval of several weeks, the produced  $^{37}\text{Ar}$  atoms are separated from the target material. Their subsequent decay via electron capture to excited levels of  $^{37}\text{Cl}$  which de-excites via Auger emission is counted in a proportional counter. Surprisingly, Davis et al. found fewer neutrino interactions than predicted by the Standard Solar Model. The deficit was confirmed by other experiments, e.g. Gallex/GNO, SAGE and Kamiokande. These observations established the solar neutrino problem. The deficit was either pointing to an incorrect solar model or the fact that the neutrinos undergo a change of flavor on their way from the center of the sun to the detection on earth. The experiments mentioned above were almost exclusively sensitive to the electron flavor type only and therefore were not able to detect neutrinos of other flavors, which are expected if neutrinos are subject to neutrino oscillations.

A similar observation, yet in the GeV energy range, was made by the Super-Kamiokande experiment [3] which measured a deficit of  $\nu_\mu$  from the atmosphere. In the atmosphere neutrinos are mainly produced via pion decay and subsequent muon decay, leading to a 2:1 ratio of  $\nu_\mu$  to  $\nu_e$ . Interestingly, the deficit of  $\nu_\mu$  was maximal for those neutrinos passing through the earth, i.e. at a maximal distance to the source.

To definitively test the neutrino oscillation hypothesis in the solar sector the Sudbury Neutrino Observatory (SNO) was built [4, 5]. SNO was designed to provide sensitivity to all neutrino flavors. In the first phase, 1,000 t of pure heavy water were used as detector medium. The  $\text{D}_2\text{O}$  target allows for elastic scattering (ES) off electrons, as well as, neutral (NC) and charged current (CC) interactions on deuterium:

$$\nu_x + e \rightarrow \nu_x + e^- \quad (\text{CC for } \nu_e \text{ only, NC for all flavors}) \quad (2.4)$$

$$\nu_e + d \rightarrow p + p + e^- \quad (\text{CC for } \nu_e \text{ only}) \quad (2.5)$$

$$\nu_x + d \rightarrow p + n + \nu_x \quad (\text{NC for all flavors}) \quad (2.6)$$

Each of the different channels gives rise to a specific signal. Therefore it is possible to measure the total neutrino flux and the electron neutrino flux separately. To validate and refine the result the fluxes were cross-checked with different detection schemes for neutrons from the NC reactions, based on pure  $\text{D}_2\text{O}$  (Phase 1), salt water (Phase 2) and  $^3\text{He}$  (Phase 3) as medium for neutron capture. It could indeed be shown that the total neutrino flux from the sun is conserved, leading to the conclusion that the neutrino flavor changes on the way from the sun to the earth. Figure 2.4 shows the flux results for  $\nu_\mu$ ,  $\nu_\tau$  and  $\nu_e$ .

## 2.2.2 Theoretical Description

The phenomenon of neutrino oscillations arises from the fact that neutrino mass eigenstates are not identical to the flavor eigenstates, i.e. the neutrino state coupling to weak interaction is not equal to the state propagating. This mixing can be considered analogous to the well-known mixing in the quark sector, where quarks however

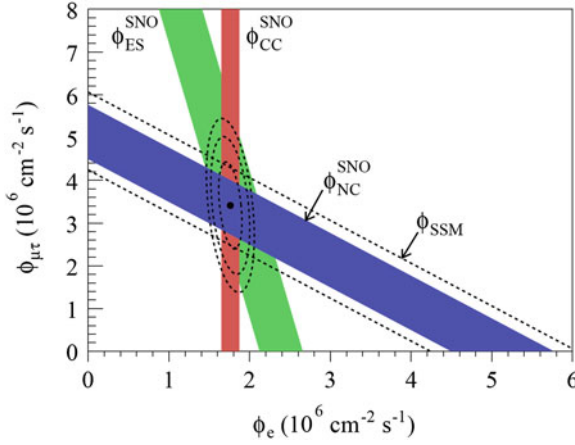


**Fig. 2.4** Flavor composition of  $^8\text{B}$  neutrinos from the sun. The *three solid bands* show the fluxes measured via different reactions in SNO. The charged current reaction (CC) determines the electron neutrino flux, while the neutral current reaction is not sensitive to the flavor and determines the total flux. The total flux is in agreement with the prediction (*dashed line*). The intersection of the CC, NC and ES bands indicates that the flux is composed of  $1/3 \nu_e$  and  $2/3 \nu_\mu$  and  $\nu_\tau$  [26]

cannot be detected as freely propagating particles due to confinement. A better comparison and analogy is thus given by the K and B meson oscillation [27].

A neutrino flavor eigenstate  $\nu_\alpha$ , with  $\alpha = e, \mu, \tau$  is defined as a superposition of neutrino mass eigenstates  $\nu_i$ , with  $i = 1, 2, 3$ .

$$\begin{pmatrix} \nu_e \\ \nu_\mu \\ \nu_\tau \end{pmatrix} = \begin{pmatrix} U_{e1}^* & U_{e2}^* & U_{e3}^* \\ U_{\mu1}^* & U_{\mu2}^* & U_{\mu3}^* \\ U_{\tau1}^* & U_{\tau2}^* & U_{\tau3}^* \end{pmatrix} \begin{pmatrix} \nu_1 \\ \nu_2 \\ \nu_3 \end{pmatrix} \quad (2.7)$$

where  $U$  is called the Pontecorvo-Maki-Nakagawa-Sakata (PMNS) matrix. It contains three mixing angles  $\theta_{ij}$  and one non-trivial complex Dirac phase ( $\delta_D$ ). In addition there are 2 complex Majorana phases ( $\delta_M$ ). The phases can cause CP violation and are of relevance in double  $\beta$ -decay. The PMNS matrix is most commonly factorized in the form

$$U = \begin{pmatrix} 1 & 0 & 0 \\ 0 & c_{23} & s_{23} \\ 0 & -s_{23} & c_{23} \end{pmatrix} \begin{pmatrix} c_{13} & 0 & s_{13}e^{-i\delta_D} \\ 0 & 1 & 0 \\ -s_{13}e^{-i\delta_D} & 0 & c_{13} \end{pmatrix} \begin{pmatrix} c_{12} & s_{12} & 0 \\ -s_{12} & c_{12} & 0 \\ 0 & 0 & 1 \end{pmatrix} \begin{pmatrix} e^{i\delta_{M1}} & 0 & 0 \\ 0 & e^{i\delta_{M2}} & 0 \\ 0 & 0 & 1 \end{pmatrix}, \quad (2.8)$$

where  $s_{ij} = \sin(\theta_{ij})$  and  $c_{ij} = \cos(\theta_{ij})$ .

Considering a case in which an electron neutrino  $\nu_e$  is produced, the state at  $t = 0$  can be written as

$$|\nu(t > 0)\rangle = |\nu_e\rangle = U_{e1}^* |\nu_1\rangle + U_{e2}^* |\nu_2\rangle + U_{e3}^* |\nu_3\rangle. \quad (2.9)$$

The mass eigenstates  $\nu_i$  are the physical states (eigenstates of the free Hamiltonian) that propagate through space with a definite energy  $E_i$  and momentum  $p_i$ . After a certain time  $t > 0$  the state evolves to

$$|\nu(t > 0)\rangle = U_{e1}^* e^{-iE_1 t} |\nu_1\rangle + e^{-iE_2 t} U_{e2}^* |\nu_2\rangle + e^{-iE_3 t} U_{e3}^* |\nu_3\rangle \neq |\nu_e\rangle. \quad (2.10)$$

This superposition of mass eigenstates is not necessarily a flavor eigenstate. Therefore one finds a non-vanishing probability to measure the neutrino in a different flavor than at origin  $t = 0$ . The neutrino is always detected in a flavor eigenstate, as it interacts only by the weak force.

Using the fact that each mass eigenstate can itself be expressed as a superposition of flavor eigenstates one can more generally express a flavor state  $\nu_\alpha$  at a time  $t$  as

$$|\nu_\alpha(t)\rangle = \sum_k U_{\alpha k}^* e^{-iE_k t} |\nu_k\rangle \quad (2.11)$$

$$= \sum_{\beta=e,\mu,\tau} \underbrace{\left( \sum_k U_{\alpha k}^* e^{-iE_k t} U_{\beta k} \right)}_{A_{\nu_\alpha \rightarrow \nu_\beta(t)}} |\nu_\beta\rangle, \quad (2.12)$$

where

$$|\nu_k\rangle = \sum_{\beta=e,\mu,\tau} U_{\beta k} |\nu_\beta\rangle \quad (2.13)$$

was used. The probability  $P$  to find a certain flavor state  $\nu_\beta$  is given by the projection of the state  $|\nu_\alpha(t)\rangle$  onto the flavor eigenstate  $|\nu_\beta\rangle$ .

$$P(\nu_\alpha \rightarrow \nu_\beta(t)) = |\langle \nu_\beta | \nu_\alpha(t) \rangle|^2 = |A_{\nu_\alpha \rightarrow \nu_\beta}(t)|^2 = \left| \sum_k U_{\alpha k}^* e^{-iE_k t} U_{\beta k} \right|^2 \quad (2.14)$$

$$= \sum_{k,j} U_{\alpha k}^* U_{\beta k} U_{\alpha j} U_{\beta j}^* e^{-i(E_k - E_j)t} \quad (2.15)$$

Using an ultra relativistic approximation with the assumption  $p_k = p = E$  one derives the following standard expression for  $P$ :

$$P(\nu_\alpha \rightarrow \nu_\beta(L/E)) = \sum_{k,j} U_{\alpha k}^* U_{\beta k} U_{\alpha j} U_{\beta j}^* e^{-i \frac{\Delta m_{jk}^2 L}{2E}} \quad (2.16)$$



with  $\Delta m_{ik}^2 = m_i^2 - m_k^2$  corresponding to the mass splittings,  $L$  denoting the distance between source and detector, and  $E$  corresponding to the energy of the neutrino. One can see that the oscillation probability  $P$  is determined by the mixing parameters of the PMNS matrix and the two mass splittings.

Since one of the three mixing angles  $\theta_{13}$  is found to be small the generic  $3\nu$  mixing case is reduced to decoupled two neutrino flavor oscillation. In that case the transition probability is simplified to the generic  $2\nu$  case:

$$P_{\nu_e \leftrightarrow \nu_\mu}(L/E) = \sin^2(2\Theta) \sin^2\left(\frac{\Delta m^2 L}{2E}\right) \quad (2.17)$$

This equation nicely shows that the amplitude of the oscillation probability  $\sin^2(2\Theta)$  depends on the corresponding mixing angle  $\Theta$ , while the mass splitting  $\Delta m^2$  determines the frequency. A more general description of neutrino oscillations, which makes no use of the ad hoc assumptions of the standard approach, is based on a quantum field theoretical wave packet model [28, 29].

### 2.2.3 Determination of Oscillation Parameters

To determine the full set of  $\nu$ -mixing parameters different neutrino sources have to be used. These include natural sources like the atmosphere and the sun, and man made sources, like reactors and accelerators. The specific  $L/E$  ratios are tuned to the mass splitting  $\Delta m^2$  and mixing angle  $\Theta$  being investigated.

Solar neutrino experiments are most sensitive to the mixing angle  $\Theta_{12}$ , also called the solar mixing angle, whereas atmospheric oscillation experiments are most sensitive to the mixing angle  $\Theta_{23}$  (atmospheric mixing angle). More recently, the main emphasis of oscillation experiments has shifted to tune the baseline of reactor or accelerator experiments to optimize the sensitivity to the unknown parameter  $\theta_{13}$ .

By adjusting the  $L/E$  ratio, an experiment can measure the oscillatory nature of the flavor transitions. A prime example, shown in Fig. 2.5, is given by the measurement results of the Kamioka Liquid Scintillator Antineutrino Detector (KamLAND) [30]. KamLAND is a long-baseline experiment at the Kamioka Laboratory in Japan. It observes reactor neutrinos at an average distance of 180 km (mean of all Japanese reactors) and is therefore measuring the “solar” mixing angle  $\Theta_{12}$ . The result nicely shows the oscillation pattern given in Eq. (2.17).

The best fit result of all current experiment is [31]:

$$\sin^2(2\Theta_{12}) = 0.87 \pm 0.03 \quad (2.18)$$

$$\Delta m_{12}^2 = (7.59 \pm 0.20) \cdot 10^{-5} \text{ eV}^2 \quad (2.19)$$

$$\sin^2(2\Theta_{23}) > 0.92 \quad (2.20)$$

$$|\Delta m_{23}^2| = (2.43 \pm 0.13) \cdot 10^{-3} \text{ eV}^2 \quad (2.21)$$

$$\sin^2(2\Theta_{13}) < 0.15 \quad (90 \% \text{ CL}) \quad (2.22)$$

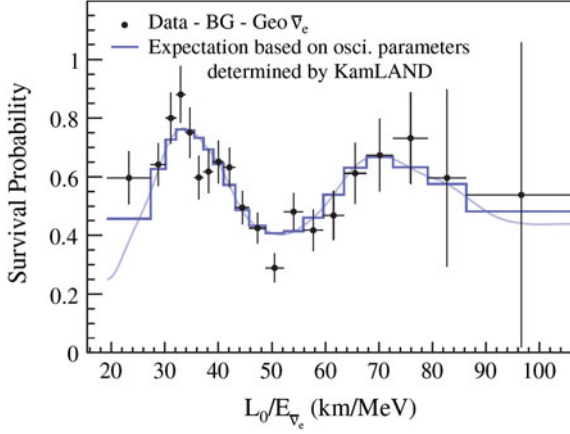


**Fig. 2.5** Result of KamLAND. Survival probability of reactor neutrinos  $\bar{\nu}_e$  as a function of distance over energy [30]. By considering different energy regimes of the neutrinos the  $L/E$  ratio is varied and an oscillation pattern becomes visible

The “atmospheric” mixing angle  $\Theta_{23}$  is almost maximal (i.e.  $45^\circ$ ),  $\Theta_{12}$  is very large and  $\Theta_{13}$  is very small. Recent results from T2K reveal a parameter space  $0.03 \text{ (} 0.04 \text{)} < \sin^2(2\Theta_{13}) < 0.28 \text{ (} 0.34 \text{)}$  for no CP violation and normal (inverted) hierarchy at 90% CL [6]. This has been corroborated by very recent results from Double Chooz [7].

For  $\Delta m_{23}^2$  only the absolute value is known, hence the generic mass hierarchy of the neutrinos is not known. Oscillations in matter are sensitive to the sign of the mass splitting, therefore the sign of  $\Delta m_{12}^2$ , as deduced from solar neutrinos travelling in solar matter, is known.

### 2.2.4 Oscillation in Matter

The oscillation pattern is changed in the presence of matter, which is described by the so-called Mikheyev-Smirnov-Wolfenstein (MSW) effect [32]. The matter of the sun consists of baryonic matter (i.e. quarks) and electrons. Elastic scattering of neutrinos off nuclei is the same for all neutrino flavors. In the elastic scattering off electrons the neutral current component is identical for neutrinos of all flavors, however, the charged current component enters only for the electron neutrino. This flavor distinction results in an effective electron neutrinos mass and hence in a modification of the oscillation pattern.

The  $\nu_e$ ’s “feel” an additional potential  $V$  that changes their energy  $E$

$$E^2 \rightarrow (E + V)^2 \approx E^2 + 2EV = E^2 + 2E\sqrt{2}G_F N_e, \quad (2.23)$$

The potential  $V$  is proportional to the Fermi constant  $G_F$  and the electron density  $N_e$ . Since the Hamiltonian is changed correspondingly, also the time evolution of a flavor state is modified. In case of solar neutrino oscillations it is sufficient to consider only two flavor oscillation between  $\nu_e$  and  $\nu_x$ , which is a superposition of  $\nu_\mu$  and  $\nu_\tau$ . Since the neutrinos are ultra-relativistic  $x = ct$ , i.e. the spatial evolution is equivalent to the time evolution, the evolution of the flavor eigenstates in vacuum is given by

$$\frac{\partial}{\partial x} \begin{pmatrix} \nu_e \\ \nu_x \end{pmatrix} = H_0 \begin{pmatrix} \nu_e \\ \nu_x \end{pmatrix} \quad (2.24)$$

$$= \frac{\Delta m_{12}^2}{2E} \begin{pmatrix} -\cos(2\Theta) & \sin(2\Theta) \\ \sin(2\Theta) & \cos(2\Theta) \end{pmatrix} \begin{pmatrix} \nu_e \\ \nu_x \end{pmatrix}. \quad (2.25)$$

Taking into account the flavor diagonal matter effect the evolution equation is changed to

$$\frac{\partial}{\partial x} \begin{pmatrix} \nu_e \\ \nu_x \end{pmatrix} = \left( \frac{\Delta m_{12}^2}{2E} \begin{pmatrix} -\cos(2\Theta) & \sin(2\Theta) \\ \sin(2\Theta) & \cos(2\Theta) \end{pmatrix} + V(x) \begin{pmatrix} 1 & 0 \\ 0 & 0 \end{pmatrix} \right) \begin{pmatrix} \nu_e \\ \nu_x \end{pmatrix}. \quad (2.26)$$

Diagonalizing the Hamiltonian gives two mass eigenstates in matter which are different from the mass eigenstates in vacuum. When solving Eq. (2.26) different cases can be distinguished:

In case the neutrino is produced at very high electron densities and its energy is large, the parameter  $\frac{\Delta m_{12}^2}{2E}$  can be neglected compared to  $V$ . The Hamiltonian takes a diagonal form and the neutrino at origin is mostly made of the heavy mass eigenstate in matter, as visualized in Fig. 2.6. Assuming a slow change of the density in the sun, the neutrino stays in the same mass eigenstate all the time (adiabaticity). As the density decreases with the radius, the neutrinos pass through a region where the matter effect and vacuum oscillation are equal, i.e. the diagonal terms in the Hamiltonian cancel and consequently the neutrino mass eigenstate is an equal admixture of both flavors (level crossing). As the density drops to zero at the solar surface the mass eigenstate in matter eventually turns into a mass eigenstate in vacuum. No further oscillations occur in vacuum since the state is a pure mass eigenstate. The probability to measure an electron neutrino on the earth is fixed and given by the projection of the mass eigenstate on the electron flavor, which is approximately 1/3 (see Fig. 2.7). If the neutrino has less than 1 MeV the matter effect can be neglected compared to the vacuum oscillation term. This energy dependence has been verified by a suite of experiments, most notably by Borexino.

## 2.3 Theory of Neutrino Mass

In the Standard Model no theoretical mechanism is foreseen to provide a mass term for neutrinos. Correspondingly, the neutrino mass is the first evidence for physics beyond the Standard Model. The fact that neutrino masses are smaller than the mass of

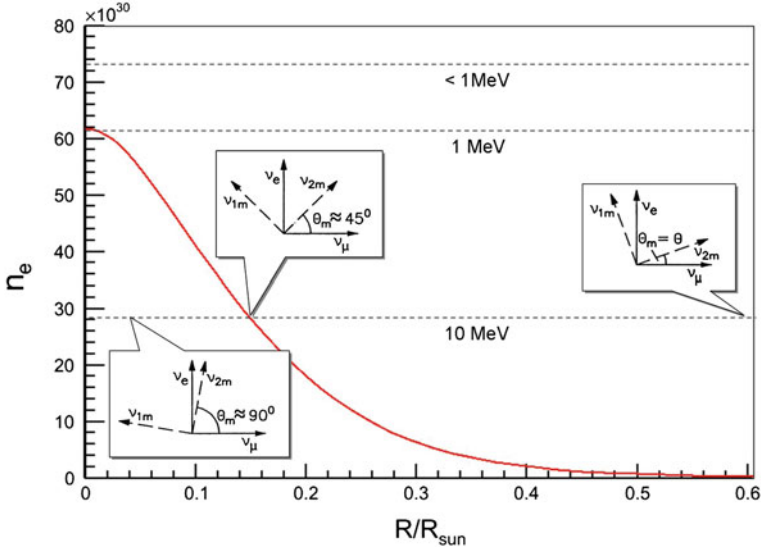


**Fig. 2.6** Visualization of MSW effect. The *red line* shows electron density per  $\text{m}^3$  as a function of solar radius. The *three horizontal lines* indicate the behavior of neutrinos of different energies in sun. For very low-energy neutrinos the matter effect can be neglected. The electron density is only relevant for neutrino energies larger than 1 MeV. For a 10 MeV  $\nu_e$ , produced in the center of the sun, the matter effect  $V$  firstly dominates the vacuum oscillation term in Eq. (2.26), i.e. the Hamiltonian is approximately diagonal. The *inset on the left* visualizes how in that case the  $\nu_e$  is mostly made up of the heavy mass eigenstate in matter  $\nu_{2m}$ . As long as the density in the sun changes adiabatically the neutrino stays in its mass eigenstate. As the neutrino moves out of the sun, it eventually crosses an area where the matter effect and vacuum oscillation are equal, i.e. the diagonal terms in Eq. (2.26) exactly cancel. The *inset in the middle* shows that the mass eigenstate in matter is an equal admixture of both flavors. Finally, when the neutrino leaves the sun, the mass eigenstate in matter is equal to the mass eigenstate in vacuum. The angle  $\Theta$  in the *inset on the right* corresponds to the vacuum mixing angle. The neutrino underwent a resonant flavor change: at production  $\nu_{2m}$  is mostly  $\nu_e$ , whereas in vacuum only  $1/3$  of  $\nu_{2m} = \nu_2$  is  $\nu_e$

the charged leptons by at least 5 orders of magnitude implicates that neutrinos acquire mass by a different mechanism than the standard Higgs mechanism. In the following possible mass terms and natural mechanisms that can explain the smallness of the neutrino mass, in particular the so-called See-Saw mechanism, will be explained.

### 2.3.1 Possible Mass Terms in the Lagrangian

To write down a neutrino mass term analogous to the electron mass term a right chiral neutrino singlet  $\nu_R$  has to be introduced to the Standard Model

$$\mathcal{L}_{\text{mass}}^D = - \sum_{l, l'} \bar{\nu}_{l'L} M_{ll'}^D \nu_{l'R} + \text{h.c.}, \quad (2.27)$$

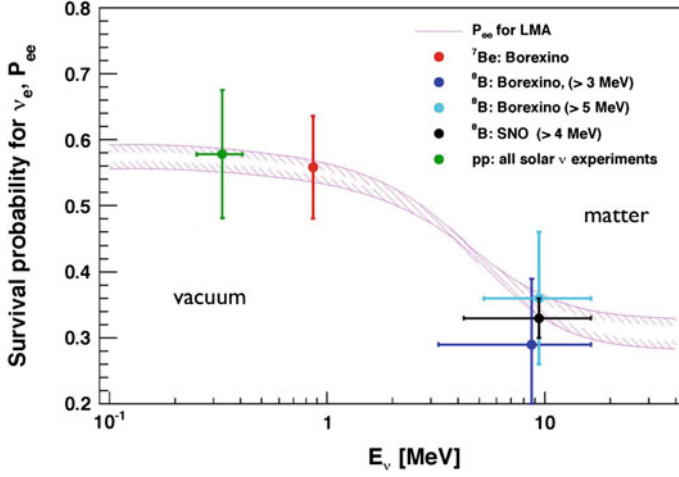


**Fig. 2.7** Survival probability of electron neutrinos from the sun as a function of their energy. The figure shows that only for neutrinos of more than approximately 1 MeV the matter effect plays a role. If the vacuum oscillation dominates the survival probability is roughly 0.5

where  $l$  and  $l'$  run over all flavors and L and R denote the chirality.  $\mathcal{L}^D$ , the so-called Dirac mass term, is realized via a coupling to the Higgs field. In this scenario, a neutrino mass of the right order of magnitude can only be achieved by fine tuning: The Yukawa coupling  $y$  has to be chosen unnaturally small to about  $y = 10^{-13}$ , which is considered not very appealing. In case the mass of the neutrino is realized in this way, the neutrino would be a so-called Dirac particle.

It is also possible to construct a mass term only from the Standard Model neutrino fields [33]

$$\mathcal{L}_{\text{mass}}^{\text{M,L}} = -\frac{1}{2} \sum_{l,l'} \bar{\nu}_{l'L} M_{ll'}^{\text{M,L}} (\nu_{lL}^C) + \text{h.c.} \quad (2.28)$$

This term violates lepton number by 2 units. If the neutrinos acquire their mass via this mechanism they are so called Majorana particles and can be considered to be their own antiparticle.

Both mass terms in Eqs. (2.27) and (2.28) must be generated with the help of a Higgsfield in order not to violate gauge invariance. However, for right chiral singlet it is possible to construct a Majorana mass term without a Higgsfield. These fields are singlets under the SU(2) gauge group and therefore such a term does not violate gauge invariance.

$$\mathcal{L}_{\text{mass}}^{\text{M,R}} = -\frac{1}{2} \sum_{l,l'} \bar{\nu}_{l'R}^C M_{ll'}^{\text{M,R}} \nu_{lR} + \text{h.c.} \quad (2.29)$$

Finally, it is also possible to introduce a neutrino mass via radiative corrections or new physics, e.g. SUSY or extra dimensions [34–37].

### 2.3.2 See Saw Mechanism

Two ways to naturally generate a small neutrino mass can be distinguished [38, 39]. A first approach is to only consider the Majorana mass term in Eq. (2.28). To couple  $(\bar{\nu}_L)^C$  and  $\nu_L$ , which both have weak isospin  $I_W^3 = +\frac{1}{2}$ , a state with weak isospin  $I_W^3 = -1$  has to be added, e.g. two Standard Model Higgs fields. This term then has mass dimension 5 and is interestingly the only possible dimension 5 operator made of only Standard Model particles. Since terms in the Lagrangian always have to be of dimension 4 in order to be renormalizable, such a term can only be introduced in an effective field theory approach. In that case, to reduce the dimension by 1, it has to be divided by a mass. This mass is naturally chosen to be of a high energy scale, e.g. of the GUT scale, thereby it suppresses the new physics associated with the dimension 5 term. The corresponding term in the Lagrangian

$$\mathcal{L}_{\text{Majorana}} = g \frac{1}{\Lambda} (\bar{\nu}_L)^C \nu_L \phi^0 \phi^0, \quad (2.30)$$

includes a coupling constant  $g$ , a large scale  $\Lambda$  and two Higgs fields  $\phi^0$ . After electro-weak symmetry breaking the Higgs field acquires a non-vanishing vacuum expectation value and a Majorana mass term is generated

$$M^M \propto \frac{1}{2} \frac{(yv)^2}{\Lambda} = \frac{m_{\text{EW}}^2}{\Lambda} \quad (2.31)$$

with  $y$  denoting the Yukawa coupling and  $v$  the vacuum expectation value of the Higgs field. Introducing a neutrino mass term via a dimension 5 operator naturally provides a small neutrino mass due to the large mass scale  $\Lambda$  in the denominator. To generate a neutrino mass of  $\propto 1$  eV, the corresponding large mass scale  $\Lambda$  must be chosen to be  $\propto 10^{13}$  GeV, which is interpreted to be the lepton number breaking scale. This mechanism does not naturally provide a hierarchy of the neutrino masses and therefore supports the degenerate mass regime of the neutrinos.

Another way to generate a small neutrino mass is with the help of the right chiral field. In that case the two mass terms in Eqs. (2.27) and (2.29) are considered. The Lagrangian can be written as

$$\mathcal{L}_{\text{mass}} = -\frac{1}{2} \bar{\nu}_L M^{\text{D+M,R}} (\nu_L)^C \quad (2.32)$$

with

$$\mathbf{v}_L = \begin{pmatrix} \nu_L \\ (\nu_R)^c \end{pmatrix}, \quad (2.33)$$

$$M^{D+M,R} = \begin{pmatrix} 0 & M^D \\ (M^D)^T & M^{M,R} \end{pmatrix} \quad (2.34)$$

When diagonalizing the mass matrix one find two mass eigenstates: a very light one  $m_1$  and a heavy one  $m_2$

$$m_1 \approx \frac{(M^D)^2}{M^{M,R}} \quad (2.35)$$

$$m_2 \approx M^{M,R} \quad (2.36)$$

As with the first mechanism (Eq. 2.31), also here small neutrino masses naturally occur. In this case also a hierarchy of neutrino masses naturally arises, due to the Dirac mass in the numerator. For a more detailed description see [40, 41].

## 2.4 Determination of the Neutrino Mass

A precise determination of the neutrino mass would have a large impact on both particle physics and cosmology. For particle physics the knowledge about the neutrino mass could give rise to a better understanding of the mass generating mechanism in nature. The role of the neutrino in cosmology depends on its actual mass scale, see Fig. 2.8. The mass of relic neutrinos in the universe can contribute sizably to the total matter content, and, moreover influence the structure formation in the early universe.

Three main approaches to measure the absolute neutrino mass scale are currently being explored: cosmological studies of the formation and evolution of large-scale structures (LSS), the search for neutrinoless double  $\beta$ -decay ( $0\nu\beta\beta$ ), and the investigation of the kinematics of single  $\beta$ -decay. It should be emphasized that all methods measure a different effective neutrino mass. In the following the main ideas of the approaches will be described and the differences will be pointed out.

### 2.4.1 Cosmology

Neutrinos play an important role on cosmological scales due to their vast abundance in the universe. From the Big Bang there are about  $336$  relic neutrinos/cm<sup>3</sup> in the entire cosmos today. Consequently, even though their mass is rather small neutrinos can contribute significantly to the total matter-energy density of the universe. However, for the total dark matter in the universe to be made of neutrinos, the sum of the neutrino masses  $m_{\nu_i}$  would have to be unrealistically large ( $\sim 30$  eV). Figure 2.8

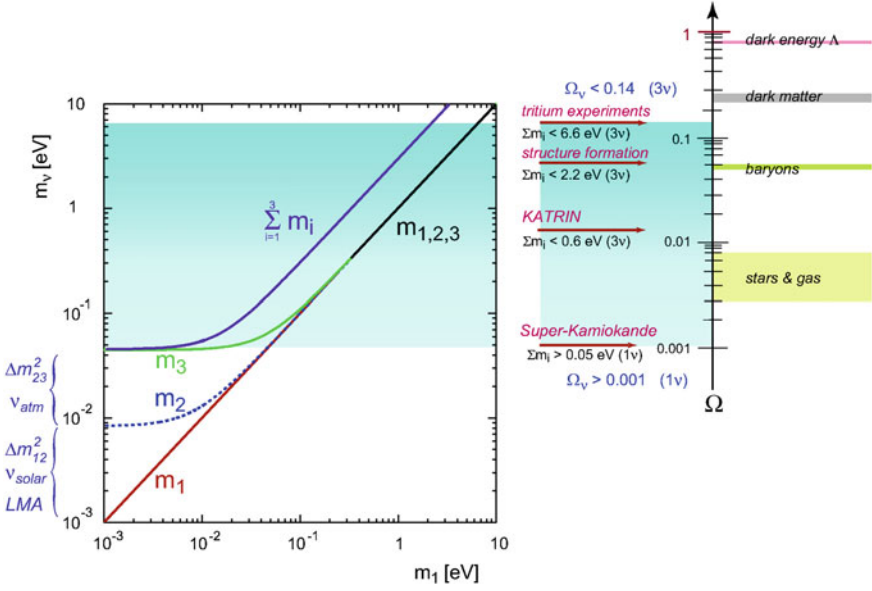


**Fig. 2.8** Neutrino contribution to the total mass in the universe. The *plot on the left* shows  $m_{\nu_i}$  as a function of the lightest neutrino mass eigenstate. From neutrino oscillation experiments the mass splittings are known, however, not the overall mass scale. Direct neutrino mass experiments give an upper bound on the absolute neutrino mass scale. Two extreme cases can be distinguished for the mass of the lightest neutrino mass eigenstate: it could be of the order of the mass splittings (hierarchical scenario) or of the order of the upper neutrino mass bound (degenerate scenario), where the mass splittings would play a minor role. Particle physics provides several models to generate a neutrino mass, some of which prefer the degenerate and others the hierarchical scenario. Consequently, by knowing the absolute neutrino mass scale one could distinguish between the scenarios and thereby promote some models over others. On the *right-hand side* of the figure, the possible contribution of the neutrino to the energy density of the universe is demonstrated. The *red arrows* indicate the experimental bounds on the neutrino mass [42]

shows the contribution to the total matter of the universe depending on the mass scale of the neutrino.

In the very early universe, at timescales of about  $1 \text{ s}$  ( $\propto 10^9 \text{ K}$ ), neutrinos experienced a “freeze-out” from thermal equilibrium. Thermal freeze-out of a particle occurs when the collision rate is smaller than the Hubble parameter, describing the rate of expansion of the universe. Since the freeze-out temperature of  $T_\nu = 1 \text{ MeV}$  is very high, neutrinos at that time were ultra-relativistic. Furthermore, since the “cooling time” of the neutrinos is very slow, they influence structure formation in the form of so-called hot dark matter. Neutrinos act as “cosmic architects” by carrying energy out of clumped matter, due to their large free-streaming length. This implies that small perturbations of the matter density are washed out by neutrinos (see Fig. 2.9). Only structures of scales larger than the free-streaming length of neutrinos of about  $1 \text{ Gpc}$  (for  $m_\nu \sim 1 \text{ eV}$ ) can thus be formed in a hot dark matter dominated universe.



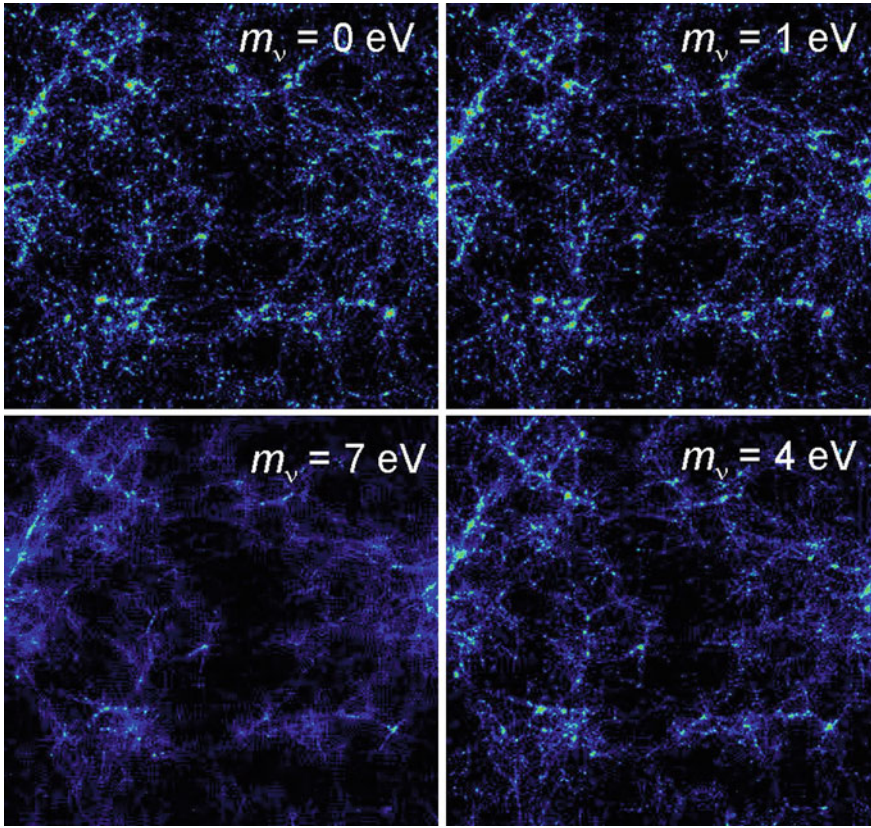


**Fig. 2.9** Influence of the neutrino mass on small-scale structures of the universe. The plots show a simulation of the structure formation for different neutrino masses. For large neutrino masses the small scales are smeared out

The matter distribution of the universe can be measured by the Cosmic Microwave Background (CMB), galaxy and galaxy cluster surveys, weak lensing, Lyman- $\alpha$ -forest and 21-cm-line measurements [43]. The amount of small structures at different cosmological epochs is sensitive to the neutrino mass. It is evident that the more heavy the neutrino is, the more effective the washing out of small-scale structures will proceed. Figure 2.10 shows the power spectrum for different neutrino masses. Cosmology is sensitive to the absolute sum of neutrinos masses

$$m(\nu) = \sum_i m_{\nu_i}. \quad (2.37)$$

The current upper limits [43] are

$$m(\nu) < 0.5 - 2 \text{ eV}. \quad (2.38)$$

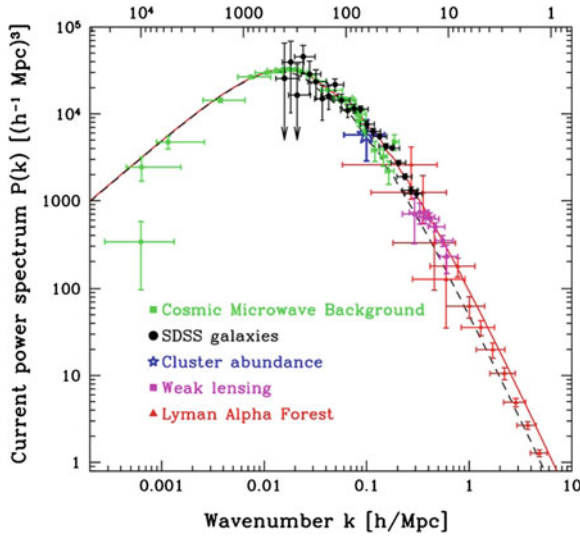


**Fig. 2.10** Influence of the neutrino mass on the matter power spectrum. This plot shows the measurements and theoretical prediction of the matter power spectrum. The *solid line* represents a standard scenario, where the neutrino mass is assumed to be zero. The *dashed line* corresponds to where neutrinos contribute with 7% to the dark matter in the universe, i.e. their mass is approximately 1 eV. The power spectrum is reduced by a factor of 2 for large wave numbers, i.e. small-scale structures [44]

The large variations are due to the fact that cosmological methods still are very model dependent and thus crucially depend on the parameter and data base being used.

### 2.4.2 Neutrinoless Double Beta Decay

A  $\beta$ -decay converting a neutron into a proton will transmute an even–even nucleus into an odd–odd nucleus, with generally less binding energy. In some cases, the daughter element with  $Z+1$  protons has therefore a higher mass excess. As a consequence, the single  $\beta$ -decay is energetically forbidden and double  $\beta$ -decay as a second order weak process becomes experimentally observable (see Fig. 2.11). In this rare decay two electrons and two neutrinos are produced simultaneously

$$2n \rightarrow 2p + 2e^- + 2\bar{\nu}_e. \quad (2.39)$$

However, if the neutrino is its own antiparticle, i.e. a Majorana particle, the neutrino produced in one of the  $\beta$ -decays can be absorbed at the other vertex. In this case, there would be no neutrino in the final state. This process is called neutrinoless double  $\beta$ -decay ( $0\nu\beta\beta$ ). In the Standard Model, which does not allow for lepton

number violation, this decay is does not occur. Observing this decay would prove the Majorana nature of the neutrino.

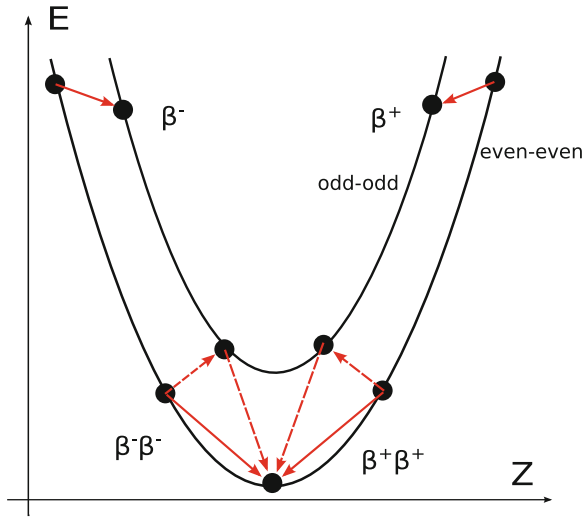
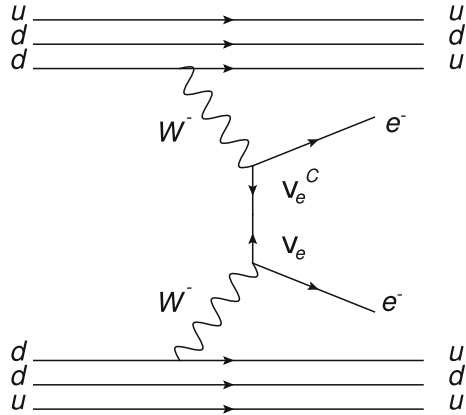


**Fig. 2.11** Mass excess  $E$  as a function of number of protons  $Z$ . This figure illustrates that in some cases the single  $\beta$ -decay is energetically forbidden. This is the case for 60 naturally occurring isotopes. However, only in seven cases double  $\beta$ -decay has been experimentally observed

**Fig. 2.12** Feynmangraph of neutrinoless double  $\beta$ -decay



The decay amplitude  $\Gamma$  depends on the neutrino mass. To find the exact dependence, one considers the Feynman graph of  $0\nu\beta\beta$  decay (see Fig. 2.12). The neutrino propagator is given by

$$\sum_i P_L U_{ei} \frac{\not{p} - m_i}{p^2 + m^2} U_{ei} P_L, \quad (2.40)$$

where  $P_L = \frac{1-\gamma^5}{2}$  is a projector on a left chiral component of a field, accounting for the fact of maximal parity violation of the weak interaction and  $U$  is the PMNS matrix. As the matrices  $\gamma^5$  and  $\gamma^\mu$  anti-commute the  $\not{p}$ -term of the propagator vanishes. The mass parameter  $m^2$  in the denominator can be neglected compared to  $p^2$ . One can then define an effective neutrino mass as

$$\Gamma \propto \langle m\beta\beta \rangle = \left| \sum_i U_{ei}^2 m_{\nu_i} \right|. \quad (2.41)$$

with  $\langle m\beta\beta \rangle$  denoting the Majorana neutrino mass.

It is important to note that  $\langle m\beta\beta \rangle$  is a coherent sum of the neutrino masses. Since the PMNS matrix contains complex phases, cancellations are possible. As a result, even for relatively large  $m_{\nu_i}$ , the contribution to  $0\nu\beta\beta$  decay could be small. Additionally, the measurement is sensitive to uncertainties of the parameters of the PMNS matrix, especially the CP violating phases. When deducing the neutrino mass from the  $0\nu\beta\beta$  decay rate one needs to take into account the fact that not only the massive Majorana neutrino contributes to the decay amplitude, but also any other corresponding physics beyond the Standard Model, e.g. right handed currents and SUSY, which can give rise to non-negligible contributions.

The experimental signature of  $0\nu\beta\beta$  decay is a mono-energetic peak produced by the sum of the energies of the two electrons in the final state. The peak coincides with the endpoint of the continuous spectrum of the dominant  $2\nu\beta\beta$  mode, as shown in Fig. 2.13. To deduce the neutrino mass from the experimental data, the lifetime  $T_{1/2}$  of the  $0\nu\beta\beta$  decay of a specific isotope is measured. The Majorana mass  $\langle m\beta\beta \rangle$  depends on the lifetime  $T_{1/2}$  and the nuclear matrix elements  $|M_{nuc}|$

$$\langle m\beta\beta \rangle^2 = \left( T_{1/2} G(Q, Z) |M_{nuc}|^2 \right)^{-1} \quad (2.42)$$

where  $G(q, Z)$  denotes the phase space factor for  $0\nu\beta\beta$  decay. The matrix elements can be computed with several methods, e.g. by a shell model ansatz, or a quasi particle random phase approximation (QRPA), etc. However, the matrix elements of  $0\nu\beta\beta$  for many nuclei are only known within an accuracy of about a factor of 2. The Heidelberg-Moscow experiment has claimed an experimental evidence for  $\langle m\beta\beta \rangle \approx 0.4 \text{ eV}$  [45]. This result is disputed in the community and needs to be scrutinized by current and future experiments like the GERmanium Detector Array (GERDA) [46], CUORE [47], Super-Nemo [48], EXO [49], and MAJORANA [50].

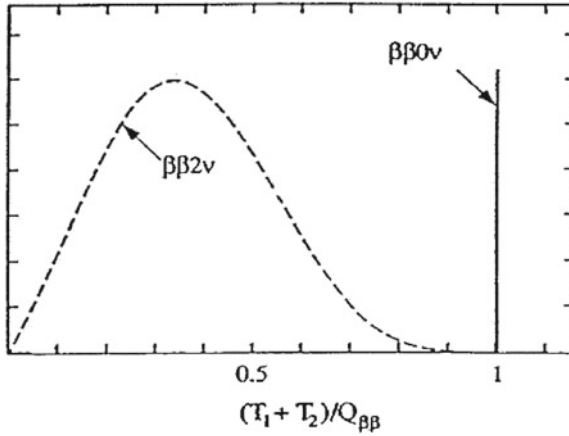


**Fig. 2.13** Experimental signature of neutrinoless double  $\beta$ -decay. The figure shows the distribution of the sum of the electron energies ( $T_1 + T_2$ ) normalized to the Q-value (mass difference of mother and granddaughter nucleus). The continuous spectrum is due to the  $2\nu\beta\beta$  decay, the monoenergetic peak is the signature of  $0\nu\beta\beta$  decay [51]

### 2.4.3 Single Beta Decay

The  $\beta^-$  decay of a nucleus is a weak decay in which a neutron is converted to a proton while an electron  $e^-$  and electron anti neutrino  $\bar{\nu}_e$  are produced:

$$(A, Z) \rightarrow (A, Z + 1) + e^- + \bar{\nu}_e \quad (2.43)$$

The kinematics of the  $\beta^-$ -decay is sensitive to the neutrino mass. A nonzero neutrino mass reduces the endpoint energy and distorts the spectrum, especially in the vicinity of the endpoint, as visualized in Fig. 2.14. The  $\beta$ -electron energy spectrum is given by

$$\frac{dN}{dE_e} = C \cdot F(E, Z) \cdot p_e \cdot (E_e + m_e c^2) \cdot (E_0 - E_e) \sum_i |U_{ei}|^2 \sqrt{(E_0 - E_e)^2 - m_{\nu_i}^2}, \quad (2.44)$$

where  $F(E, Z)$  corresponds to the Fermi function, taking into account the Coulomb interaction of the outgoing electron with the daughter nucleus. The variables  $p_e$ ,  $E_e$  and  $m_e$  are the electron momentum, kinetic energy and mass, respectively and  $E_0$  is the endpoint energy for zero neutrino mass. Correspondingly,  $E_0 - E_e$  is the total energy of the neutrino. The momentum of the neutrino is given by the sum of the momenta of each mass eigenstate, weighted by their fraction  $|U_{ei}|^2$  within the electron flavor. The constant  $C$  is given by

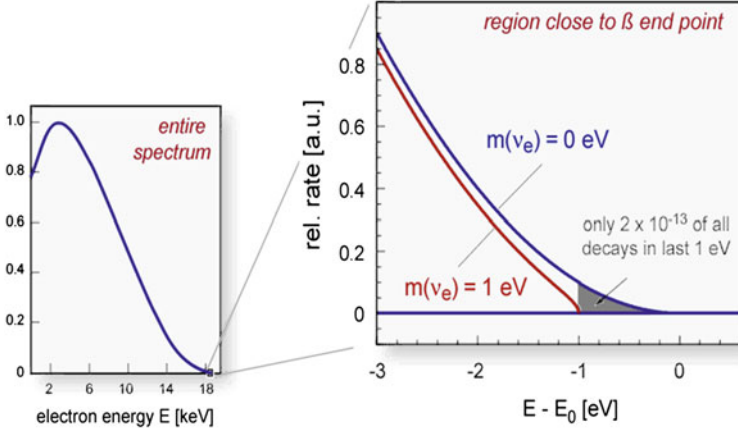


**Fig. 2.14** Tritium  $\beta$  spectrum close to the endpoint. *Left* Full tritium spectrum. *Right* Zoom into the region close to the endpoint

$$C = \frac{G_F^2}{2\pi^3} \cos^2 \Theta_C |M|^2. \quad (2.45)$$

with  $G_F$  being the Fermi constant and  $\Theta_C$  the Cabbibo angle accounting for the transition strength of a down quark into an up quark (change of neutron into a proton).  $|M|^2$  is the nuclear matrix element. In case of a super-allowed transition  $|M|^2$  is not energy dependent close to the endpoint and therefore does not influence the shape of the spectrum.

For the region  $(E_0 - E_e)^2 \ll m_{\nu_i}^2$  Eq. (2.44) can be expanded to

$$\frac{dN}{dE_e} \approx C \cdot F(E, Z) \cdot p_e(E_e + m_e c^2) (E_0 - E_e)^2 \sum_i |U_{ei}|^2 \left( 1 - \frac{1}{2} \frac{m_{\nu_i}^2}{(E_0 - E_e)^2} \right) \quad (2.46)$$

$$= C \cdot F(E, Z) \cdot p_e(E_e + m_e c^2) \left( (E_0 - E_e)^2 - \frac{1}{2} \sum_i |U_{ei}|^2 m_{\nu_i}^2 \right) \quad (2.47)$$

$$= C \cdot F(E, Z) \cdot p_e(E_e + m_e c^2) (E_0 - E_e) \sqrt{(E_0 - E_e)^2 - \sum_i |U_{ei}|^2 m_{\nu_i}^2} \quad (2.48)$$

The expression  $\sum_i |U_{ei}|^2 m_{\nu_i}^2 =: \langle m_\beta \rangle^2$  is called the “effective electron antineutrino mass”. In principle, a super-high resolution analysis of the spectrum would be sensitive to the single mass eigenstates. However, the experimental precision in  $\beta$ -spectroscopy does not allow to resolve the tiny mass splittings and therefore the

effective electron neutrino mass  $\langle m_\beta \rangle^2$  is measured.  $\langle m_\beta \rangle^2$  is an incoherent sum of the neutrino masses, meaning that in contrast to the  $0\nu\beta\beta$  method no cancellations can occur. Furthermore, the single  $\beta$ -decay is not sensitive to the intrinsic nature of the neutrino, i.e. whether it is a Majorana or Dirac particle.

In a measurement of the  $\beta$ -spectrum all parameters that modify the spectrum, such as electronic final states, recoil energy of the daughter nucleus and radiative corrections need to be taken into account. To be sensitive to neutrino masses in the cosmologically preferred sub-eV range, one needs an instrument with a very good energy resolution, high luminosity and very low background. The current experimental limit from analysis of tritium  $\beta$ -decay is  $\langle m_\beta \rangle < 2$  eV from the Mainz and Troitzk experiments [8–11].

These experiments have pioneered high precision  $\beta$ -spectroscopy of molecular tritium with the so-called MAC-E filter technique [52, 53]. However, due to limitations in the experimental resolution  $\Delta E$ , and, more importantly, due to limits of the source intensity, the sensitivity of both experiments did not allow to explore the sub-eV range. In the following chapter the design principles and criteria of the next-generation tritium  $\beta$ -decay experiment KATRIN will be presented, which allows to push the precision in  $\beta$ -spectroscopy to unprecedented levels.

## References

1. R. Davis, A review of the homestake solar neutrino experiment. *Prog. Part. Nucl. Phys.* **32**, 13–32 (1994)
2. B. Cleveland, T. Daily, R.D. Jr., J. Distel, K. Lande, C. Lee, P. Wildenhain, J. Ullman, Update on the measurement of the solar neutrino flux with the homestake chlorine detector. *Nucl. Phys. B Proc. Suppl.* **38**(1–3), 47–53 (1995). *Neutrino 94*
3. Y. Fukuda et al., Evidence for oscillation of atmospheric neutrinos. *Phys. Rev. Lett.* **81**, 1562–1567 (1998)
4. Q.R. Ahmad, Direct evidence for neutrino flavor transformation from neutral-current interactions in the sudbury neutrino observatory. *Phys. Rev. Lett.* **89**, 011301 (2002)
5. Q.R. Ahmad, Measurement of the rate of  $\nu_e + d \rightarrow p + p + e^-$  interactions produced by  $B8$  solar neutrinos at the sudbury neutrino observatory. *Phys. Rev. Lett.* **87**, 071301 (2001)
6. K. Abe et al., Indication of electron neutrino appearance from an accelerator-produced off-axis muon neutrino beam. *Phys. Rev. Lett.* **107**, 041801 (2011)
7. H.D. Kerrect, First results from the Double Chooz experiment, in *LowNu 2011* (2011)
8. C. Kraus, B. Bornschein, L. Bornschein, J. Bonn, B. Flatt, A. Kovalik, B. Ostrick, E.W. Otten, J.P. Schall, T. Thümmeler, C. Weinheimer, Final results from phase II of the Mainz neutrino mass search in tritium. *Eur. Phys. J. C* **40**, 447–468 (2005)
9. J. Bonn, B. Bornschein, L. Bornschein, L. Fickinger, B. Flatt, O. Kazachenko, A. Kovalik, C. Kraus, E.W. Otten, J.P. Schall, H. Ulrich, C. Weinheimer, The mainz neutrino mass experiment. *Nucl. Phys. B Proc. Suppl.* **91**(1–3), 273–279 (2001). *Neutrino 2000*
10. V.M. Lobashev, V.N. Aseev, A.I. Belev, A.I. Berlev, E.V. Geraskin, A.A. Golubev, O.V. Kazachenko, Y.E. Kuznetsov, R.P. Ostroumov, L.A. Rivkis, B.E. Stern, N.A. Titov, S.V. Zadorozhny, Y.I. Zakharov, Direct search for mass of neutrino and anomaly in the tritium beta-spectrum. *Phys. Lett. B* **460**(1–2), 227–235 (1999)
11. V.M. Lobashev, V.N. Aseev, A.I. Belev, A.I. Berlev, E.V. Geraskin, A.A. Golubev, O.V. Kazachenko, Y.E. Kuznetsov, R.P. Ostroumov, L.A. Rivkis, B.E. Stern, N.A. Titov,



- C.V. Zadoroghny, Y.I. Zakharov, Direct search for neutrino mass and anomaly in the tritium beta-spectrum: Status of troitsk neutrino mass experiment. *Nuclear Physics B - Proceedings Supplements* **91**(1–3), 280–286 (2001). *Neutrino 2000*
12. J. Chadwick, Intensitätsverteilung im magnetischen Spektrum von  $\beta$ -Strahlen von Radium B+C. *Verh. d. Deutsch. Phys. Ges.* **15**, 383 (1914)
  13. W. Pauli, Letter to Gauvereinstagung in Tübingen: “Sehr geehrte radioaktive Damen und Herren”, published in R. Kronig and V. Weisskopf (Eds.), Wolfgang Pauli, *Collected scientific Papers*, Vol. 2, Interscience, New York (1964), 1930.
  14. E. Fermi, Versuch einer Theorie der  $\beta$ -Strahlen. *Z. Phys. A: Hadrons Nucl.* **88**, 161–177 (1934). doi:[10.1007/BF01351864](https://doi.org/10.1007/BF01351864)
  15. F.A. Scott, Energy spectrum of the  $\beta$ -rays of radium E. *Phys. Rev.* **4** (1935)
  16. C.L. Cowan, F. Reines, F.B. Harrison, H.W. Kruse, A.D. McGuire, Detection of the free neutrino: a confirmation. *Science* **124**(3212), 103–104 (1956)
  17. F. Reines, C.L. Cowan, F.B. Harrison, A.D. McGuire, H.W. Kruse, Detection of the free anti-neutrino. *Phys. Rev.* **117**, 159–173 (1960)
  18. J.-M. Gaillard, K. Goulianos, L.M. Lederman, N. Mistry, M. Schwartz, J. Steinberger, G. Danby, Observation of high-energy neutrino reactions and the existence of two kinds of neutrinos. *Phys. Rev. Lett.* **9**, 36–44 (1962)
  19. K. Kodama, Observation of tau neutrino interactions. *Phys. Lett. B* **504**(3), 218–224 (2001)
  20. D. DeCamp et al., A precise determination of the number of families with light neutrinos and of the Z boson partial widths. *Phys. Lett. B* **235**(3–4), 399–411 (1990)
  21. D. DeCamp et al., Determination of the number of light neutrino species. *Phys. Lett. B* **231**(4), 519–529 (1989)
  22. J.N. Bahcall, A.M. Serenelli, S. Basu, New solar opacities, abundances, helioseismology, and neutrino fluxes. *Astrophys. J. Lett.* **621**(1), L85 (2005)
  23. Borexino homepage. <http://borex.lngs.infn.it/>. Last update: 01 Jul 2010
  24. G. Bellini et al., Precision measurement of the  $^{7}\text{Be}$  solar neutrino interaction rate in borexino. *Phys. Rev. Lett.* **107**, 141302 (2011)
  25. Homepage of J. Bahcall. <http://www.sns.ias.edu/jnb/>. Last update: 2005
  26. B. Aharmim et al., Determination of the  $\nu_e$  and total  $B\bar{B}$  solar neutrino fluxes using the sudbury neutrino observatory phase I data set. *Phys. Rev. C* **75**, 045502 (2007)
  27. B. Kayser, B-meson and neutrino oscillation: a unified treatment. arXiv:1110.3047v1 [hep-ph]
  28. C. Giunti, C.W. Kim, J.A. Lee, U.W. Lee, On the treatment of neutrino oscillations without resort to weak eigenstates. *Phys. Rev.* **D48**, 4310–4317 (1993)
  29. C. Giunti, Neutrino wave packets in quantum field theory. *JHEP* **11**, 017 (2002)
  30. S. Abe et al., Precision measurement of neutrino oscillation parameters with KamLAND. *Phys. Rev. Lett.* **100**, 221803 (2008)
  31. K. Nakamura, P.D. Group, Review of particle physics. *J. Phys. G: Nucl. Part. Phys.* **37**(7A), 075021 (2010)
  32. L. Wolfenstein, Neutrino oscillations in matter. *Phys. Rev. D* **17**, 2369–2374 (1978)
  33. E. Majorana, Teoria simmetrica dell elettrone e del positrone. *Il Nuovo Cimento* (1924–1942) **14**, 171–184 (1937). doi:[10.1007/BF02961314](https://doi.org/10.1007/BF02961314)
  34. S. Antusch, M. Drees, J. Kersten, M. Lindner, M. Ratz, Neutrino mass operator renormalization in two Higgs doublet models and the MSSM. *Phys. Lett. B* **525**(1–2), 130–134 (2002)
  35. N. Arkani-Hamed, S. Dimopoulos, G. Dvali, J. March-Russell, Neutrino masses from large extra dimensions. *Phys. Rev. D* **65**, 024032 (2001)
  36. J. Casas, J. Espinosa, A. Ibarra, I. Navarro, Nearly degenerate neutrinos, supersymmetry and radiative corrections. *Nucl. Phys. B* **569**(1–3), 82–106 (2000)
  37. E. Ma, Verifiable radiative seesaw mechanism of neutrino mass and dark matter. *Phys. Rev. D* **73**, 077301 (2006)
  38. M. Gell-Mann, P. Ramond, R. Slansky, Complex spinors and unified theories. Prepared for Supergravity Workshop (Stony Brook, New York, 1979)
  39. R.N. Mohapatra, G. Senjanović, Neutrino masses and mixings in gauge models with spontaneous parity violation. *Phys. Rev. D* **23**, 165–180 (1981)



40. G. Altarelli, K. Winter, *Neutrino Mass*. Springer Tracts in Modern Physics (Springer, 2003)
41. R.N. Mohapatra, Theory of neutrinos: a white paper. Rep. Prog. Phys. **70**(11), 1757 (2007)
42. K. Collaboration, KATRIN Design Report (FZKA Report 7090), Tech. Rep., KIT (2004)
43. S. Hannestad, Neutrino physics from precision cosmology. Prog. Part. Nucl. Phys. **65**(2), 185–208 (2010)
44. M. Tegmark, Cosmological neutrino bounds for non-cosmologists. Phys. Scr. **2005**(T121), 153 (2005)
45. H.V. Klapdor-Kleingrothaus, A. Dietz, H.L. Harney, I.V. Krivosheina, Evidence for neutrinoless double beta decay. Mod. Phys. Lett. **A16**, 2409–2420 (2001)
46. GERDA homepage. <http://www.mpi-hd.mpg.de/gerda/>. Last update: 04 Nov 2010
47. M. Sisti, The Cuore collaboration, From cuoricino to CUORE: investigating neutrino properties with double beta decay. J. Phys.: Conf. Ser. **203**(1), 012069 (2010)
48. Super-Nemo homepage. <http://nemo.in2p3.fr/supernemo/>. 30 Oct 2006
49. Exo-200 homepage. <http://www-project.slac.stanford.edu/exo/>. 12 Sep 2011
50. Majorana homepage. <http://majorana.npl.washington.edu/>. 04 June 2009
51. R. Beuselinck, J. Sedgbeer, Y. Shitov, The supernemo experiment. <http://www.imperial.ac.uk/research/hep/research/supernemo.htm>. Last update: 2011
52. V.M. Lobashev, P.E. Spivak, A method for measuring the electron antineutrino rest mass. Nucl. Instrum. Methods Phys. Res., Sect. A **240**(2), 305–310 (1985)
53. A. Picard, H. Backe, H. Barth, J. Bonn, B. Degen, T. Edling, R. Haid, A. Hermanni, P. Leiderer, T. Loeken, A. Molz, R. Moore, A. Osipowicz, E. Otten, M. Przyrembel, M. Schrader, M. Steininger, C. Weinheimer, A solenoid retarding spectrometer with high resolution and transmission for keV electrons. Nucl. Instrum. Methods Phys. Res., Sect. B **63**(3), 345–358 (1992)

Background Processes in the Electrostatic  
Spectrometers of the KATRIN Experiment

Mertens, S.

2014, XVI, 196 p. 116 illus., 108 illus. in color.,  
Hardcover

ISBN: 978-3-319-01176-9